Chemical Engineering Journal 163 (2010) 143–153

Contents lists available at ScienceDirect

Chemical Engineering Journal

journal homepage: www.elsevier.com/locate/cej

Elimination of die swell and instability in hollow fiber spinning process of hyperbranched polyethersulfone (HPES) via novel spinneret designs and precise spinning conditions

Natalia Widjojo[a], Tai-Shung Chung[a,*], Davis Yohanes Arifin[a], Martin Weber[b], Volker Warzelhan[b]

[a] Department of Chemical and Biomolecular Engineering, National University of Singapore, 10 Kent Ridge Crescent, Singapore 117602, Singapore
[b] Polymer Research Engineering Plastics, BASF Aktiengesellschaft, GKT/B-B1, Ludwigshafen 67056, Germany

ARTICLE INFO

Article history:
Received 7 May 2010
Received in revised form 10 July 2010
Accepted 21 July 2010

Keywords:
Linear polyethersulfone
Hyperbranched polyethersulfone
Spinneret designs
Flow stability
Die swell
Spinning parameters

ABSTRACT

This study has successfully demonstrated that a proper combination of novel spinneret designs and spinning parameters can effectively counteract the die swell as well as flow instability phenomena, i.e. extrudate distortion, in the hyperbranched polyethersulfone (HPES) hollow fiber spinning. Attempts are also made to unravel the die swell and flow behavior differences between HPES and linear polyethersulfone (LPES) membranes spun using various spinneret designs and spinning conditions. In terms of flow stability, it is revealed that short conical spinnerets with a flow angle of 60° as well as short round flow channel spinneret with a flow angle of 30°, can reduce or eliminate extrudate distortions. Apart from spinneret designs, this study also accentuates the importance of a proper choice of spinning conditions for each specific spinneret to achieve flow stability and reduce die swell, namely: (1) bore fluid composition; (2) dope flow rate; (3) spinning temperature; and (4) take-up speed. Experimental results concluded that a proper combination of spinneret design and these four spinning parameters is the key to stabilize the spinning process. It is found that a high take-up speed spinning and a high non-solvent concentration in the bore fluid can fully eliminate die swell and enhance flow stability in the HPES hollow fiber spinning using short and conical or round spinnerets.

1. Introduction

The importance of hollow fiber spinning technology for vast membrane applications has been well recognized for decades. To date, both melt and solution spinning are the most widely implemented techniques in hollow fiber membrane fabrication [1–13]. Due to the complexity of spinning processes, the understanding of material rheology and its flow behavior through an orifice die are utmost critical to obtain desirable hollow fiber membranes at a reasonable production rate. Clearly, from an economical point of view, the fiber's production rate is one of the major parameters to determine maximum production capacity and profitability in the membrane industry. However, limitations caused by instabilities in the polymer flow will lead to technical problems within the production line itself or fabricate undesirable final products which possess the potential to increase production costs. Thus, advances in spinning technology and knowledge on polymeric materials are the keys to overcome the instability problem.

Some of the issues encompassed within the fiber spinning instability include: (1) draw resonance; (2) necking; (3) capillary break-up; (4) irregular cross-section and (5) melt fracture or extrudate distortion [14–21]. The first four phenomena, which have been investigated previously by many researchers [4,14,15], most likely lead to fiber breakage during the spinning process or generate a non-uniform cross-sectional diameter along the spun fibers. It is believed that their mechanisms are exacerbated by the fluctuations in polymer jet flows, which are themselves resultant of drawing or capillary forces.

The last type of spinning instability, which will be the focus of this manuscript, normally takes place in the form of a distorted, gross or wavy polymer flow [14–16]. The first melt fracture instability was investigated by Nason who observed a wavy polystyrene extrudate at Reynolds numbers in the range of 800–1000 [22]. In fact, the mechanism of extrudate distortion in melt spinning is one of the most controversial issues in fiber spinning and has been heavily debated among rheological scientists [5,14–17,23]. It can be summarized that the proposed mechanisms of extrudate distortion implicate one or more of the following parameters [15]: (1)

* Corresponding author. Tel.: +65 6516 6645; fax: +65 6779 1936.
E-mail address: chencts@nus.edu.sg (T.-S. Chung).

1385-8947/$ – see front matter © 2010 Elsevier B.V. All rights reserved.
doi:10.1016/j.cej.2010.07.048

fracture; (2) Reynolds turbulence; (3) thermal effects; (4) die entry and exit effects; (5) rheological effects; and (6) slip at the die wall. As a rule of thumb, most researchers agree that the distortions of polymer extrudate most likely appear when the recoverable shear s_R, which is defined as the ratio of the die wall shear stress to the elastic shear modulus, reaches a critical value of 1–10 [14,15]. Therefore, any effort to reduce or completely eliminate the distortions in the polymer flow must take into consideration some major parameters when spinning hollow fibers from a polymer solution, namely: (1) spinneret designs; (2) dope solution flow rate and rheology; (3) spinning temperature; (4) air gap distance; and (5) take-up speed.

Apart from the technical related parameters, the extrudate flow behavior is very much depending on the polymer material characteristics. In particular, the extrusion behavior of linear and branched polymers with nearly identical viscosity functions demonstrates major qualitative flow distinctions [5,24–26]. Generally, polymers tend to relax by motion along their backbones. However, in the branched polymers, this motion is hindered by branch points, thus the relaxation time increases dramatically [27]. The magnification of polymer chain relaxation time can possibly amplify flow instability and also can be a major contributor to the die swell effect [24,25]. For reader's information, the term flow instability used in the later discussion in this manuscript refers to the extrudate distortion behavior.

In the recent years, polymers with highly branched structures are gaining more popularity due to their large number of functional groups and high surface reactivity in contrast to their linear analogues [28]. Among the various classes of branched polymers, hyperbranched materials, an outgrowth of the invention of dendrimer, are considerably new materials, and little is known of their rheological properties [27]. Although much progress has been achieved in the structural understanding and the synthesis of hyperbranched polymers, much of the fundamental understanding, especially the industrial application of these hyperbranched polymers are still in a stage of infancy [28–30]. In addition, few studies were conducted to systematically compare hyperbranched polymer properties with their linear analogues [31], but the differences between hollow fiber membranes spun with the linear and hyperbranched counterparts were not clearly indicated. The hyperbranched polymers possessing higher intrinsic solubility, lower melt or solution viscosity and lower entanglement in their structures have been expected to be easier to process [32], which is extremely important for hollow fiber membrane spinning in large scale.

Our group conducted an investigation previously [24,25] to identify the unique properties of hyperbranched polyethersulfone (HPES) as compared to linear polyethersulfone (LPES). Rheological studies on the molten HPES and LPES materials show that HPES has a larger molecular weight and a wider molecular weight distribution compared to its linear analogue. Furthermore, the rheological characterization reveals that the HPES dope solution has a longer relaxation time than its linear counterpart. Hence, the HPES nascent fiber spun with conventional straight spinnerets shows a more pronounced die swell and flow instability, i.e. flow distortion, occurring at the spinneret's exit.

Although the residence time of a polymer solution flowing through the annular channel of spinneret (a few millimeters long) is very short, the flow-induced shear stress can affect the rheological behavior of the polymeric solution, i.e. relaxation time, die swell effect, and molecular orientation [8,25,33–37]. For straight annular spinnerets, the highest shear stress usually occurs along the die wall since the dope solution is normally a polymeric non-Newtonian fluid [38]. Therefore, it is crucial to understand the design principles behind engineering a spinneret for spinning a hyperbranched polymer for improved flow stability and reduced die swell effect. To the present, membrane researchers have attempted to modify their spinneret designs for multiple purposes, namely: (1) to tailor pore size distribution and control pure water permeability of ultrafiltration hollow fiber membranes by fabricating spinnerets with different flow angles [8]; (2) to approximately double the surface area of hollow fiber membrane for gas separation by designing a spinneret with microfabricated inserts to create corrugated patterns in the outer fiber perimeter [20]; (3) to induce interlayer diffusion in the interface of dual-layer hollow fiber membrane in order to eliminate delamination [39].

Based on the fundamental understanding of relaxation mechanism in the HPES polymer, other than the common spinneret with a L (die length)/ΔD (die channel) ratio of approximate 10, we have fabricated various other spinnerets with modified exit channels to reduce shear rate (stress) towards polymer solution inside the spinneret. Furthermore, the flow and shear behaviors inside the common and modified spinneret designs were simulated. In this regard, our objectives are: (1) to extensively examine and compare the effects of spinning parameters on the die swell effect and flow stability of LPES and HPES polymer solutions; (2) to overcome the die swell and flow instability problem with the aid of modified spinneret designs, particularly in the HPES hollow fiber membrane fabrications. It is believed that the fundamental knowledge obtained in this study not only provides useful guidelines for academia and industries in fabricating hollow fiber membranes from hyperbranched polymers but also introduces state-of-art spinneret designs to counteract die swell and flow instability in fiber spinning.

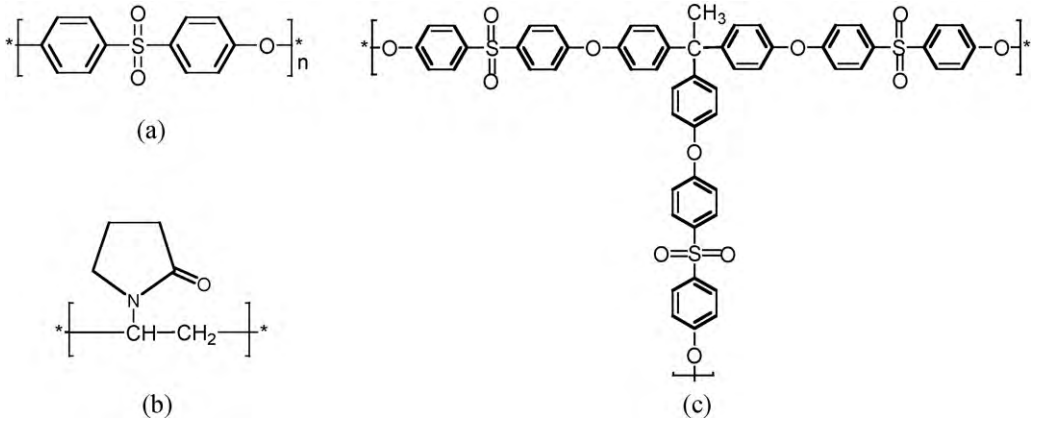

Fig. 1. The chemical structures of: (a) linear polyethersulfone (LPES); (b) hyperbranched polyethersulfone (HPES); (c) polyvinylpyrrolidone (PVP).

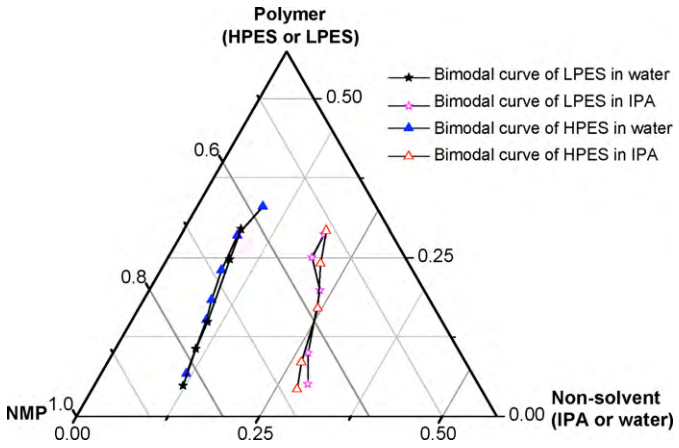

Fig. 2. Polymer/NMP/non-solvent ternary phase diagram [24].

2. Experimental

2.1. Materials

LPES (Ultrason® E6020P, Ultrason is a registered trademark of BASF SE) composed of 100 mol% linear unit and HPES composed of 2 mol% branching unit and 98 mol% linear unit were kindly supplied by BASF SE, Germany. Their chemical structures were shown in Fig. 1.

N-methyl-2-pyrrolidone (NMP) (Merck, Singapore), isopropanol (IPA) (Merck, Singapore) and polyvinylpyrrolidone (PVP) (Merck, Singapore) with an average M_w of 360,000 Da were employed as a solvent, coagulant, and additive, respectively, for hollow fiber membrane spinning.

2.2. Characterization of rheological properties of spinning solutions

The physicochemical properties, phase diagrams, molecular weights, shear viscosity and relaxation at low shear rates of LPES and HPES polymers have been studied by Yang et al. [24,25]. In summary, they have very similar melt points, thermal degradation temperatures, and contact angles. Fig. 2 describes the bimodal curves of LPES and HPES polymer solutions in the presence of non-solvent, i.e. water and IPA [24]. Interestingly, these two materials exhibit very similar phase diagrams. However, HPES has a larger molecular weight and a wider molecular weight distribution compared to its linear analogue. As a result, the HPES dope solution has a longer relaxation time than its linear counterpart at low shear rates.

The shear viscosity at high shear rates (up to 15,000 s^{-1}) of LPES and HPES polymer solutions was measured by a capillary rheometer SMART RHEO 2000 from CEAST. The diameter of the capillary dies was 1 mm and the lengths of capillary dies are 10 mm and 30 mm. The elongational viscosity was calculated according to the method proposed by Cogswell based on the measurements of pressure drop as a function of flow rate for a polymer melt or solution flowing through a thin capillary die [40].

2.3. Spinning process of hollow fiber membranes

The LPES and HPES polymer solutions at a composition of 16/10/74 wt% (polymer/PVP/NMP) were prepared following Yang et al.'s work [24]. A dry-jet wet spinning process was conducted with detailed spinning conditions listed in Table 1. The dope solution and bore fluid were extruded at a specified flow rate through a spinneret using two ISCO syringe pumps. The nascent fibers exiting from the spinneret were snapshot by a Canon EOS 350D digital camera equipped with a micro lens (MP-E 65 mm f/2.8 1–5×). A more detailed spinning procedure has been described elsewhere [24].

Table 1
Spinning parameters of HPES and LPES hollow fiber membranes.

Spinning parameter	Condition
Dope composition (wt%)	16/10/74 (polymer/PVP/NMP)[a]
Dope flow rate (ml/min)	1;2;3;4;5
Bore fluid composition (wt%)	0/100; 30/70; 55/45; 80/20; 95/5 (NMP/water)
Bore fluid flow rate (ml/min)	1.5
Air gap length (cm)	20
External coagulant (wt%)	Pure IPA
Spinning temperature (°C)	25; 60; 80
Humidity (%)	60
Take-up speed (m/min)	5.8 (free fall); 8 m/min
Spinneret	Common spinneret 0; modified 1; modified 2; modified 3; modified 4

[a] Polymers are HPES or LPES.

In this work, other than using a common straight spinneret with an $L/\Delta D$ ratio of ~10, spinnerets with various exit channel designs described in Fig. 3 were utilized. In the fiber spinning process, the purpose of having a $L/\Delta D$ ratio of ~10 in the conventional spinneret design as shown in Fig. 3a is to achieve a steady shear and fully developed flow [41,42]. However, this spinneret is not suitable for hyperbranched polymers because it promotes a long relaxation time in the nascent fiber after exiting from the long annular flow channel. Consequently, it can induce a more pronounced die swell and distorted flow caused by an incomplete polymer chain relaxation as elaborated in the later section. Therefore, we have designed four modified spinnerets with a reduced shear stress as shown in Fig. 3b–e to encounter the aforementioned problems. Modified spinneret 1 was to reduce shear experience, while modified spinneret 2 was fabricated with an enlarged channel to induce further polymer chain relaxation inside the spinneret channel. Modified spinnerets 3 and 4 were designed with a 60° converging channel and 30° round channel, respectively to shorten the flow length and minimize shear rate induced molecular orientation inside the spinneret.

2.4. Computational fluid dynamics (CFD) simulation

The commercial computational fluid dynamics (CFD) package Fluent 6.3.26 (ANSYS Inc.) was used to simulate the polymer solution flow through the spinneret. Each fluid domain of four different spinneret configurations (as shown in Fig. 3a–e) was reconstructed and meshed by the software package of Gambit 2.3 (ANSYS Inc.). All the dimensions were exactly the same as used in the experiments. Mesh was kept uniform with the maximum size of 0.1 mm to ensure accurate results.

The flow was assumed to be axisymmetric and follow the Navier Stokes equation, which is valid due to the nature of spinneret geometry. The polymer solution was assumed to be homogenous with density and viscosity of 1.5 g/cm^3 and 19.11 Pa s, respectively. The boundary conditions were set as the following. The inlet was defined at a flow rate of 2 ml/min, while the outlet was applied as the pressure outlet boundary at constant atmospheric pressure. Axis boundary condition was also applied at the centre symmetry line.

The shear rate of the fluid was calculated locally as spatial function throughout the spinneret geometry as the following:

$$\gamma = \sqrt{\frac{1}{2}\bar{\bar{e}} : \bar{\bar{e}}} \quad (1)$$

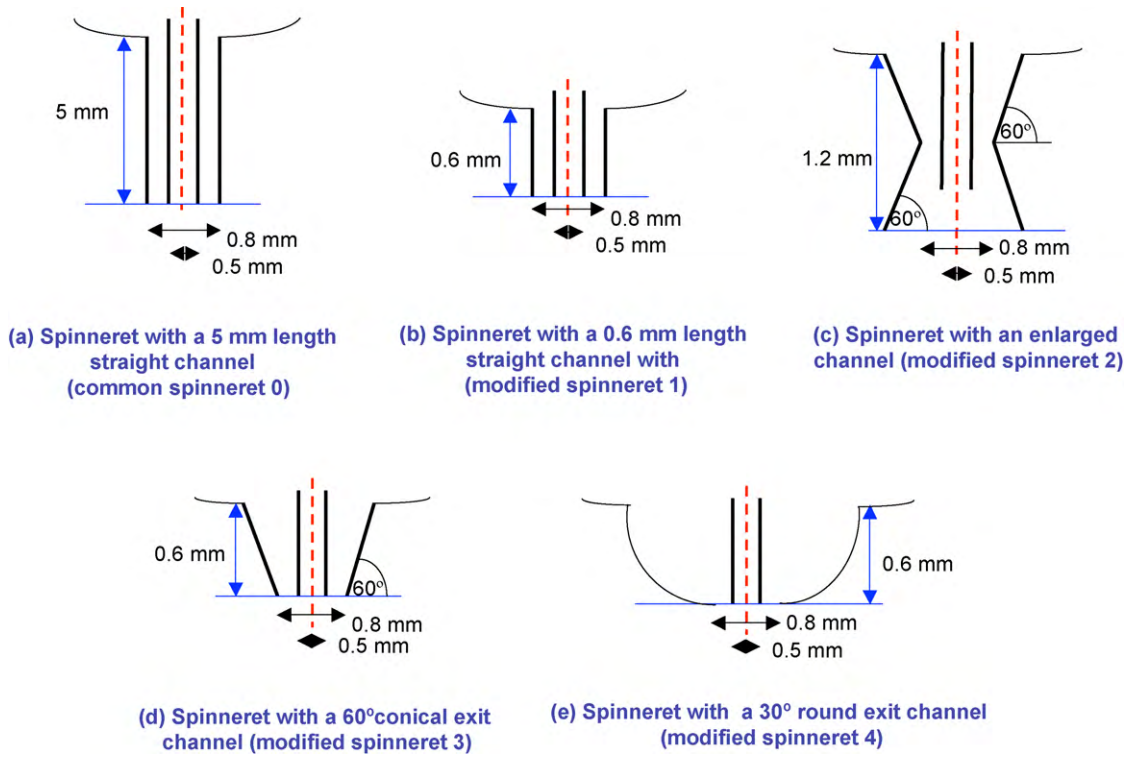

Fig. 3. The exit channel designs of common spinneret and four different modified spinnerets.

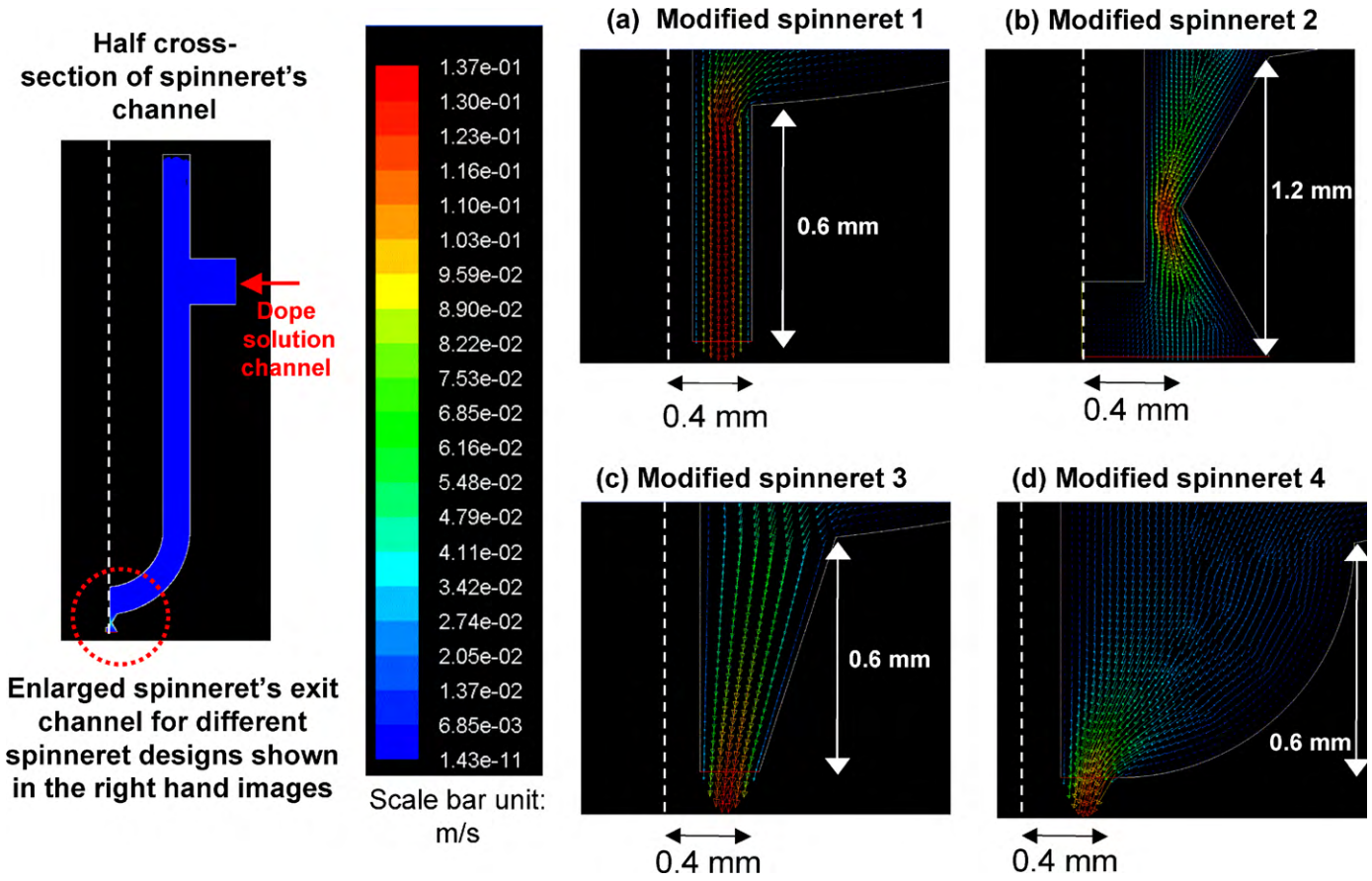

Fig. 4. Simulated velocity profile near the exit channel of different spinneret designs: (a) modified spinneret 1; (b) modified spinneret 2; (c) modified spinneret 3; (d) modified spinneret 4 (the dope's viscosity, density and flow rate of 19.11 Pa s, 1.5 g/cm^3 and 2 ml/min, respectively, were applied as the boundary conditions in this simulation).

Here, $\bar{\bar{e}}$ is the symmetric tensor for the rate of fluid strain element. For a Newtonian fluid with axisymmetric property in cylindrical coordinate, $\bar{\bar{e}}$ is defined as the following:

$$e_{ij} = \begin{bmatrix} 2\frac{\partial u_r}{\partial r} & \left(\frac{\partial u_r}{\partial \theta} + \frac{\partial u_\theta}{\partial r}\right) & \left(\frac{\partial u_z}{\partial r} + \frac{\partial u_r}{\partial z}\right) \\ \left(\frac{\partial u_r}{\partial \theta} + \frac{\partial u_\theta}{\partial r}\right) & 2\frac{\partial u_\theta}{\partial \theta} & \left(\frac{\partial u_\theta}{\partial z} + \frac{\partial u_z}{\partial \theta}\right) \\ \left(\frac{\partial u_z}{\partial r} + \frac{\partial u_r}{\partial z}\right) & \left(\frac{\partial u_\theta}{\partial z} + \frac{\partial u_z}{\partial \theta}\right) & 2\frac{\partial u_z}{\partial z} \end{bmatrix} \quad (2)$$

The tensors include the normal strain effects, represented by the diagonal terms, as well as the strains due to the shearing effects.

3. Results and discussion

3.1. The effects of spinneret designs on die swell and flow stability of LPES and HPES polymer solutions

The die swell can be considered as a consequence of the memory effect exhibited by a non-Newtonian polymeric fluid, and this phenomenon has been investigated extensively by many researchers [7,43–45]. In fact, the extrudate swell behavior through a short channel depends on both the material characteristics (linearity, molecular weight, molecular weight distribution and elasticity) and the die geometry. In this section, LPES and HPES polymer solutions with similar dope viscosity were extruded through spinnerets with various die designs. The polymer solution velocity profile through the various die designs was simulated using Matfluent 6.3 and Gambit 2.0 software as shown in Fig. 4. The velocity profile for the spinneret 0 (i.e., the common straight spinneret) is not shown because its pattern is similar to that of spinneret 1. It shows that the dope solution extruded through spinnerets 0 and 1 has the highest velocity among other spinneret designs, particularly in the centre region, which in turn affects polymer chain orientation and relaxation of the extruded polymer solution. This will be discussed more details in the following sections.

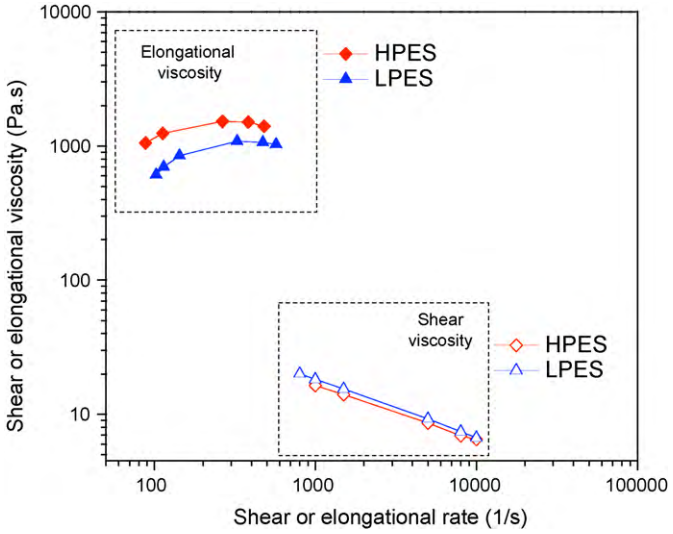

Fig. 5. The comparison of shear and elongational viscosities as a function of shear and elongational rates of LPES and HPES dope solutions.

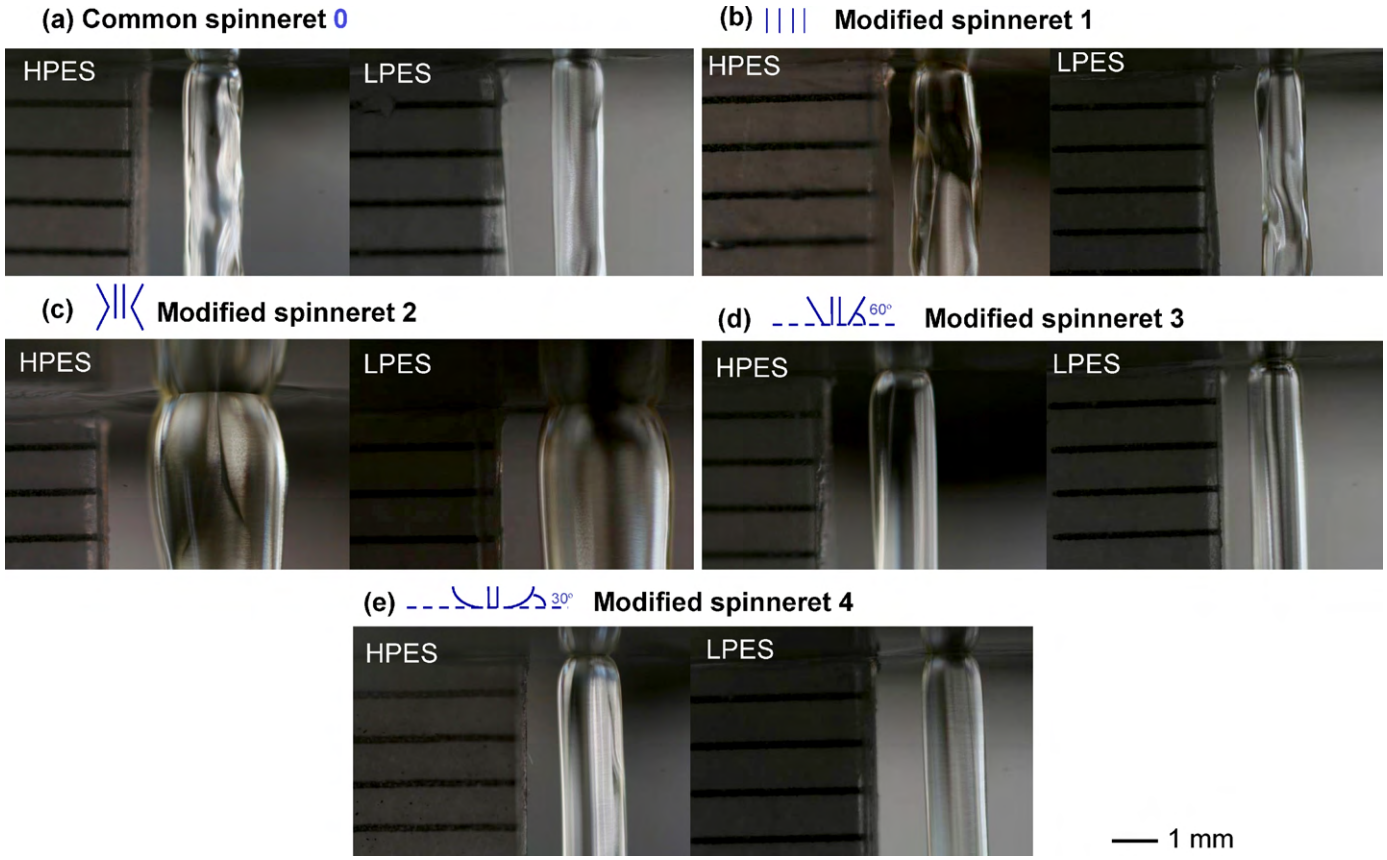

Fig. 6. Comparisons of die swell and flow stability in the HPES and LPES polymer dope solutions spun with common and modified spinnerets (a) common spinneret 0; (b) modified spinneret 1; (c) modified spinneret 2; (d) modified spinneret 3; (e) modified spinneret 4. Dope flow rate: 2 ml/min, bore fluid composition: 55/45 wt% NMP/water; take-up speed: free fall.

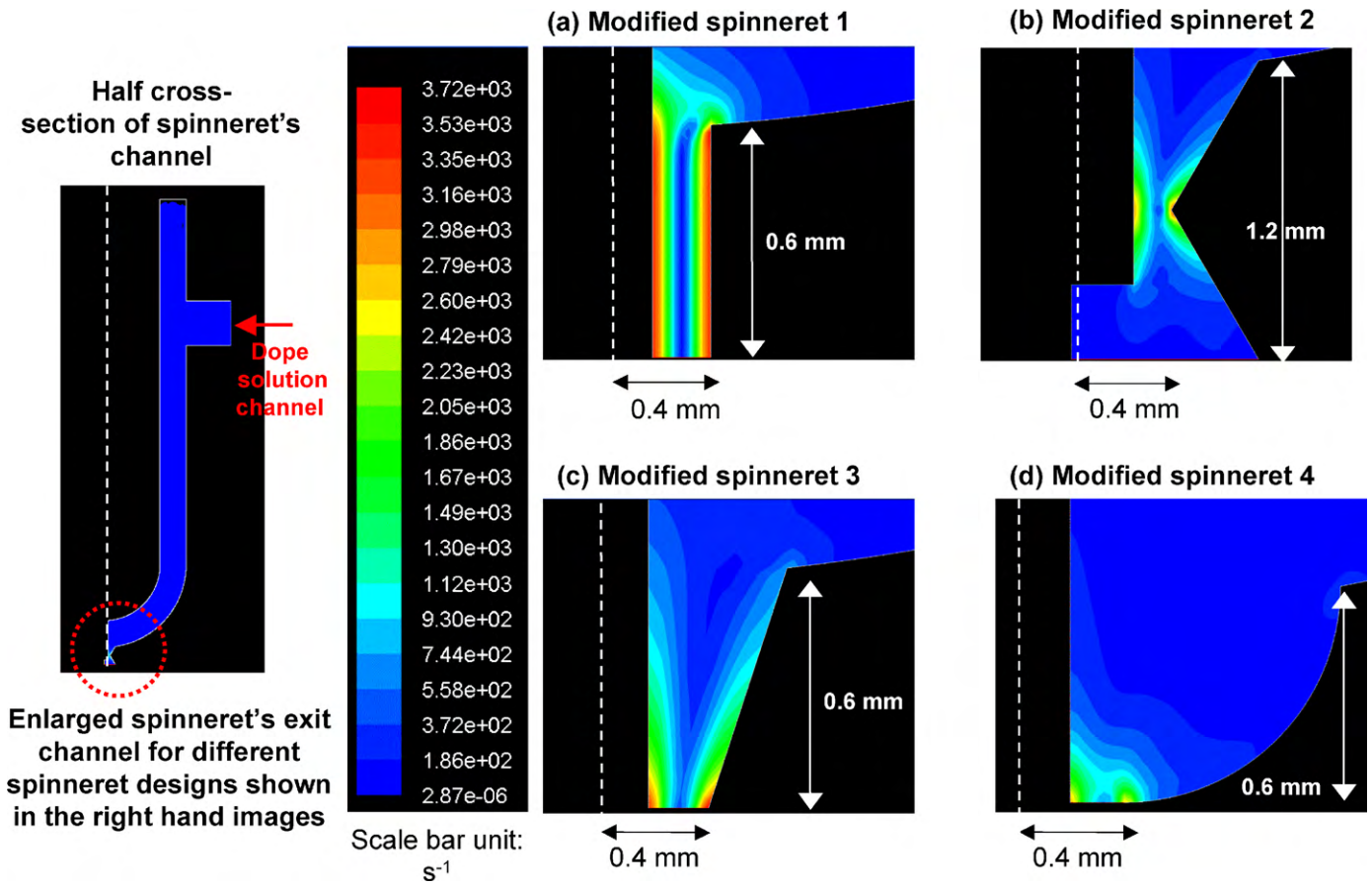

Fig. 7. Simulated shear rate profile near the exit channel of different spinneret designs: (a) modified spinneret 1; (b) modified spinneret 2; (c) modified spinneret 3; (d) modified spinneret 4 (the dope's viscosity, density and flow rate of 19.11 Pa s, 1.5 g/cm^3 and 2 ml/min, respectively, were applied as the boundary conditions in this simulation).

Fig. 5 shows the rheological properties of HPES and LPES dope solutions in terms of shear and elongational viscosities. Both dope solutions show shear and strain thinning behavior over the shear and elongational rates tested. Furthermore, it is interesting to notice that LPES and HPES dope solutions exhibit similar shear viscosity. However, the HPES dope solution has a significantly higher elongational viscosity as compared to that of LPES which consequently results in different chain alignments and relaxation responses when extruding from the spinneret. A higher elongational viscosity in HPES solutions also can be indirectly related to a longer relaxation time which has been reported previously by Yang et al. [24]. According to their observation, the HPES/PVP/NMP dope solution (the same composition as this work) exhibits a longer characteristic relaxation time (τ = 12.02 s) than that of LPES/PVP/NMP dope (τ = 8.96 s) which was calculated from dynamic frequency tests at 1% strain at room temperature [24]. Clearly, HPES requires a longer time to return its random coil chains as compared to that of LPES when extruded through the spinneret during the spinning process. Based on the aforementioned hyperbranched polymer properties, several modified spinnerets with different shapes of exit channels were designed to reduce the degree of chain alignment and facilitate chain relaxation which can significantly improve flow behavior and stability of extruded nascent hollow fibers.

Fig. 6 shows the typical die swell phenomenon during polymer extrusion via various spinneret designs. Generally, the HPES solution has a larger die swell in comparison with the LPES solution because of its higher entanglement density and normal stress [46]. The more pronounced curvature in the HPES nascent fiber could be explained by its slower relaxation development after leaving the spinneret due to its longer chain re-entanglement time or longer characteristic relaxation time [24].

In comparison among spinneret designs, modified spinneret 2 results in the most pronounced die swell for both LPES and HPES polymer solutions. This is because the polymer solution experiences more relaxation in the enlarged channel of modified spinneret 2 before contacting with the bore fluid. On the contrary, the inner structure of fibers in the other spinneret designs has been partially fixed by the bore fluid once exiting from the spinneret channel due to the rapid phase separation in the lumen-side. Hence, it retards the flexibility of polymer chain to relax which in turn can minimize the die swell effect.

In view of flow stability, Fig. 6 presents that modified spinneret 1 results in more pronounced flow instability as compared to that of common one. This may be due the fact that modified spinneret 1 might not be able to accomplish a fully developed steady state shear flow due to a shorter die length, thus the combination of chain relaxation and unsteady state flow may magnify the flow instability.

Among all spinneret designs, it appears as if that the flow stability is enhanced in modified spinnerets 2, 3 and 4 in comparison with that of the common spinneret and modified spinneret 1. Table 2 describes the mean value of hollow fiber dimensions spun using common and modified spinneret. It can be seen that common spinneret and modified spinneret 1 are likely to have a broader variation on the fiber diameter and thickness as compared to those of modified spinneret 2, 3, and 4 which further confirms our visual observation on the flow instability in common spinneret and modified spinneret 1. This enhancement in flow stability may be

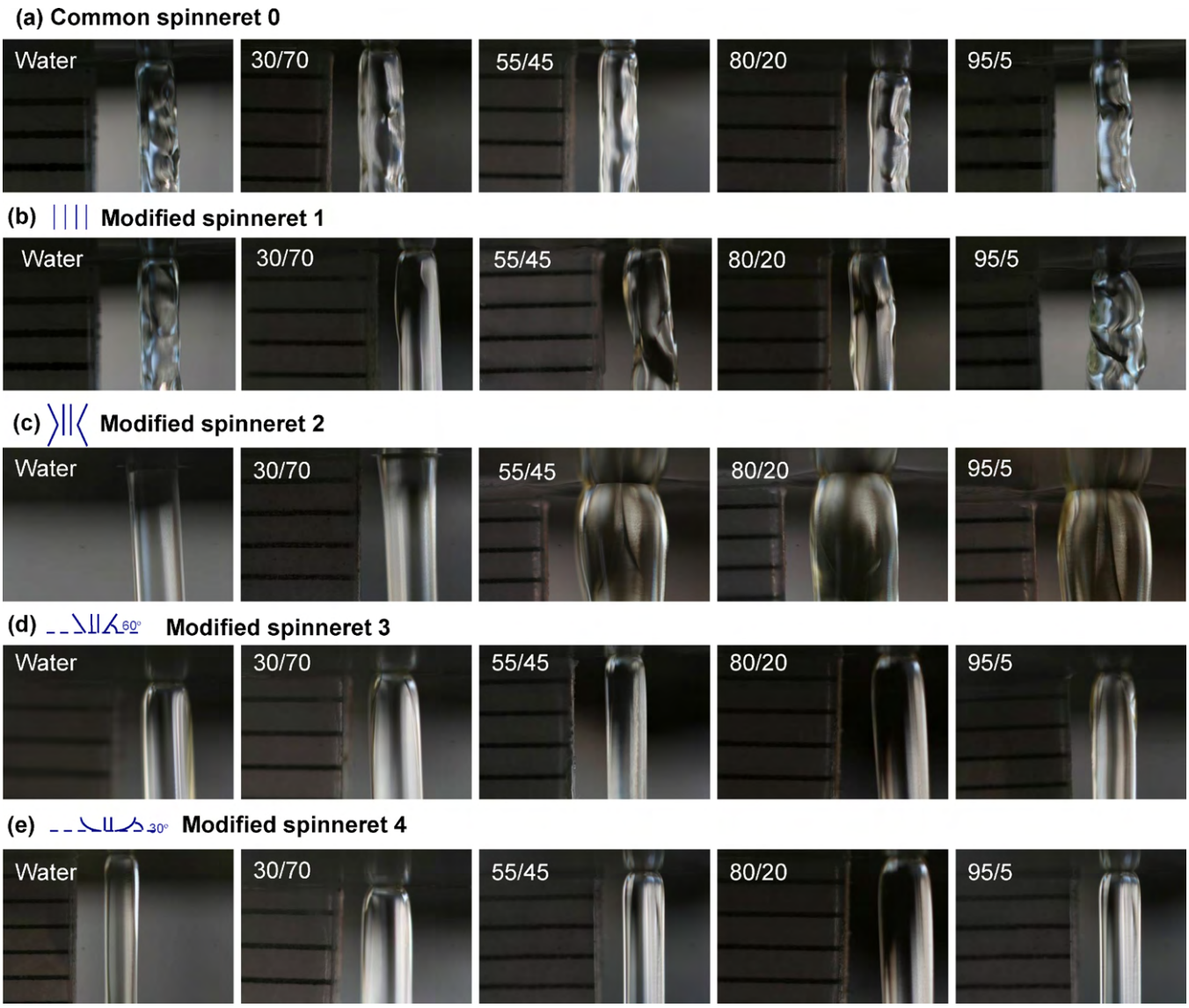

Fig. 8. The effects of bore fluid compositions (water; 30/70 NMP/water; 55/45 NMP/water; 80/20 NMP/water; and 95/5 NMP/water) on the die swell and flow stability of HPES hollow fiber spinning (a) common spinneret; (b) modified spinneret 1; (c) modified spinneret 2; (d) modified spinneret 3; (e) modified spinneret 4. Dope flow rate: 2 ml/min; take-up speed: free fall.

attributed to the modified die geometry in the exit channels of modified spinnerets 2, 3 and 4 which generate a reduced shear stress and a compression flow as simulated in Fig. 7. The reduced shear stress may decrease molecular orientation and memory, while the compression flow with the aid of lumen-side phase precipitation may stabilize the flow. Interestingly, modified spinneret 2 facilitates an additional chain relaxation through its diverging flow channel before the bore fluid is in touch with the lumen-side of fiber and initiates phase separation. This is coherent with the infinitesimal shear rate profiles near the exit channel of modified spinneret 2 as observed in Fig. 7b. As a result, there is no much resistance for chain relaxation after exiting the die and the die swell phenomenon is therefore magnified.

Based on the spinneret design, the most pronounced die swell to the least one can be ranked in the sequence of modified spinneret 2 > common spinneret 0 = modified spinneret 1 = modified spinneret 3 = modified spinneret 4. Furthermore, the order of the flow behavior in the spinneret from unstable to stable can be ranked as follows: modified spinneret 1 > common spinneret 0 > modified spinneret 2 > modified spinneret 3 = modified spinneret 4. In short,

Table 2
The mean value of hollow fiber dimensions spun using common and modified spinneret.

Spinneret ID	OD (μm)[a]	% Deviation	ID (μm)[a]	% Deviation	Thickness (μm)[a]	% Deviation
Common	1024 ± 38	3.71%	744 ± 36	4.84%	168 ± 34	20.00%
Modified 1	1080 ± 56	5.19%	792 ± 42	5.25%	164 ± 36	21.46%
Modified 2	1520 ± 42	2.76%	1190 ± 42	2.35%	186 ± 16	8.60%
Modified 3	1176 ± 24	2.04%	868 ± 22	2.53%	184 ± 18	9.78%
Modified 4	1146 ± 14	1.24%	858 ± 19	2.26%	174 ± 16	9.20%

Each mean value is calculated from five measurements.

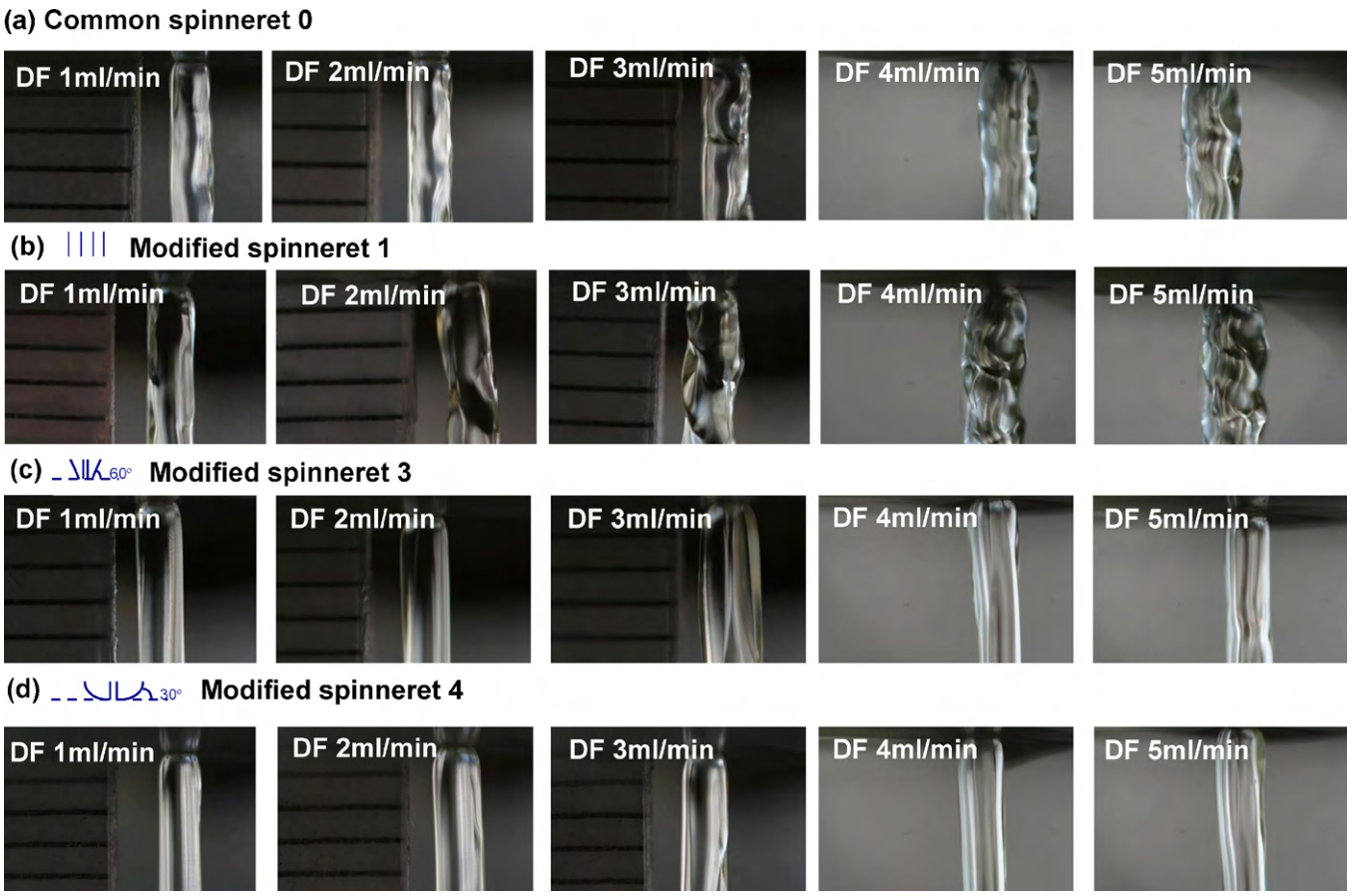

Fig. 9. The effects of dope flow rate (1, 2, and 3 ml/min) on the die swell and flow stability of HPES hollow fiber spinning (a) common spinneret; (b) modified spinneret 2; (c) modified spinneret 3; (d) modified spinneret 4. Bore fluid: 55/45 NMP/water; take-up speed: free fall.

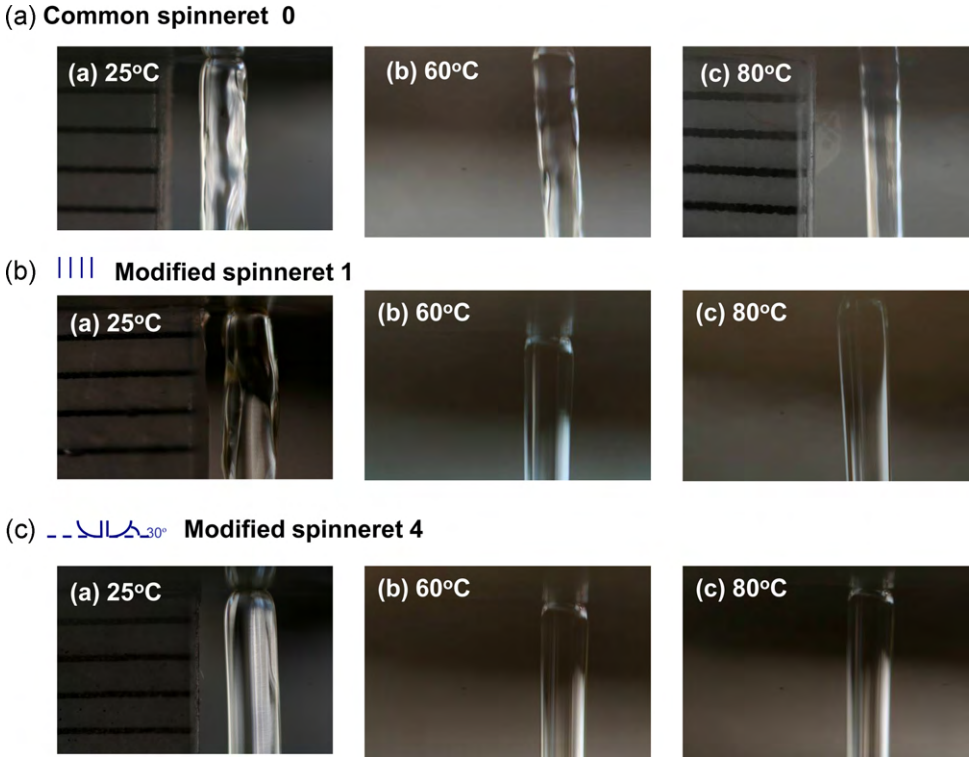

Fig. 10. The effects of spinning temperature on the die swell and flow stability of HPES hollow fiber spinning using common spinneret: (a) 25 °C; (b) 60 °C; (c) 80 °C. Dope flow rate: 2 ml/min; take-up speed: free fall; bore fluid: 55/45 NMP/water.

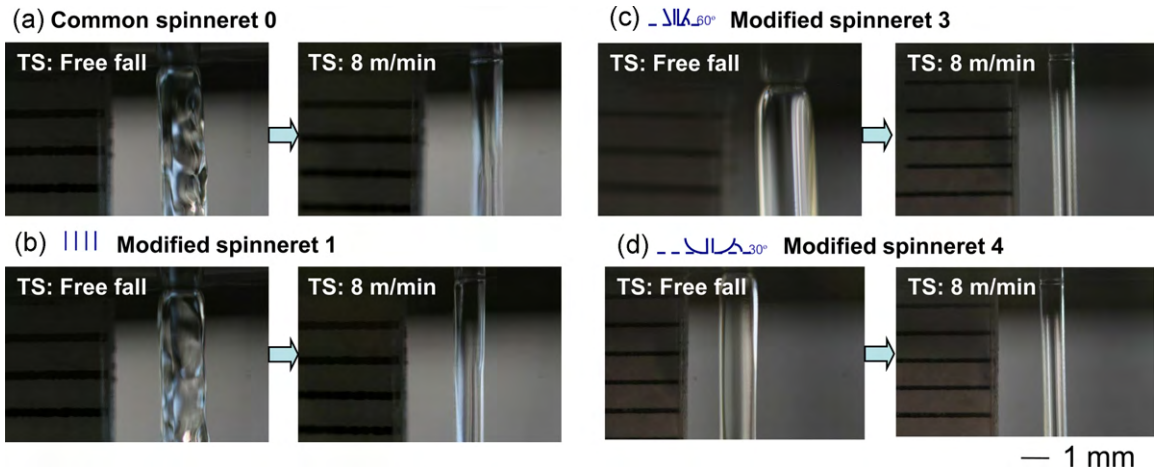

Fig. 11. The effects of increasing take-up speed (free fall to 8 m/min) on the die swell and flow stability of HPES hollow fiber spinning spun using: (a) common spinneret; (b) modified spinneret 2; (c) modified spinneret 3; (d) modified spinneret 4. Bore fluid: 55/45 NMP/water; dope flow rate: 2 ml/min.

the origin of improved flow stability may stem from the reduced overall shear stress and enhanced compression stress in combination with the lumen-side phase precipitation in the spinnerets 3 and 4.

3.2. The effects of bore fluid composition and dope flow rate on die swell and flow stability of HPES hollow fiber spinning

Fig. 8 depicts the effects of bore fluid composition on the die swell and flow stability of HPES spinning process. Surprisingly, flow instability in the extrusion of HPES dope solution can be observed in all ranges of bore fluid composition for fibers spun with common spinneret 0 and modified spinneret 1.

However, an interesting finding can be noticed in these two spinnerets. A more pronounced flow instability in the extruded HPES dope solution can be observed when the content of solvent (NMP) in the bore fluid increases from 55 to 95 wt%. This phenomenon is partially due to the slower precipitation rate induced by the NMP solvent. In comparison, the flow instability noticeably increases when the NMP content in the bore fluid reduces from 55 to 0 wt%. It is indicative of the fact that a low or no solvent concentration in the bore fluid leads to a significantly faster precipitation rate, which in turn is the resultant of forming a fiber with two different surfaces, where the inner surface has solidified but the outer surface remains in its viscous solution phase. Consequently, this results in a different relaxation rate between the lumen and shell sides of fibers which facilitates distorted flow. Hence, it can be inferred that there is a critical bore fluid composition to achieve a relatively better flow stability during fiber spinning using common spinneret and modified spinneret 1.

In view of die swell effect, the bore fluid composition seems to have a little or no effect on the die swell in the HPES extrusion using common spinneret or modified spinnerets 1, 3 and 4. However, in the modified spinneret 2, a pronounced die swell observed at the HPES extrusion spun with bore fluid 95/5 wt% NMP/water. However, this severe die swell and flow distortion can be significantly eliminated when the bore fluid composition reduces to 100 wt% water. Clearly, the chain relaxation under a constrained boundary within the diverging section and the bore fluid chemistry play important roles on the die swell and flow stability of modified spinneret 2. When the bore fluid chemistry is pure water or 70% water, the rapid precipitation can clearly suppress the relaxation and stabilize the flow because the previous relaxation under a constrained boundary within the diverging section may already remove most of the flow stress and memory. On the other hands, spinnerets 3 and 4 demonstrate stable flows in various bore fluid compositions. This suggests that designing spinnerets with proper geometry may provide an effective solution to subdue this instability phenomenon.

In conjunction, the effects of dope flow rate on the die swell and flow instability were further investigated. It is found that the die swell and flow instability behavior become more apparent when the polymer dope flow rate increases from 1 to 5 ml/min as shown in Fig. 9. Although the residence time of a polymer solution flowing through the annular channel is very short, the flow-induced stresses can affect the rheological behavior of the polymeric solution because most highly concentrated polymeric solutions are viscoelastic non-Newtonian fluids [8,38]. Consequently, a higher dope flow rate generates a higher stress inside the spinneret which results in a larger degree of die swell as well as flow instability. Therefore, the die swell and flow instability in the HPES hollow fiber spinning process can be reduced by decreasing the polymer dope flow rate with the aid of a proper spinneret design and the optimal bore fluid composition.

3.3. The effects of spinning temperature and take-up rate on die swell and flow stability of HPES hollow fiber spinning

In the literatures, high temperature spinning of polymeric solutions has been utilized to achieve diversified objectives in the hollow fiber fabrication, namely: (1) to increase production speed and produce finer fibers because of the low polymer solution viscosity at high temperatures; (2) to attain a less defective selective skin layer when the volatile non-solvent or solvent is incorporated in the spinning dope solution [11]; (3) to eliminate delamination phenomenon in the dual-layer hollow fiber membranes by enhanced interlayer diffusion [39,47]. The notable decrease in shear and elongational viscosities at high temperatures implies a dramatic loss in polymer chain entanglement and a fast relaxation rate of polymer chains, both of which could overshadow the shear/elongation induced polymer chain orientation along the spinneret channel [35–37,48]. Hence, it can subdue the die swell effect as well as enhance flow stability. Fig. 10 represents the effects of spinning temperature on die swell and flow instability of HPES hollow fiber membranes spun with a common spinneret 0, modified spinnerets 1 and 4 which confirm our hypothesis. Both die swell and flow instability significantly lessen with increasing spinning temperature.

Another viable approach to reduce die swell and flow instability can be done by adjusting the take-up speed. The take-up speed in the fiber spinning is a crucial parameter which plays an important role on hollow fiber dimension and morphology because of

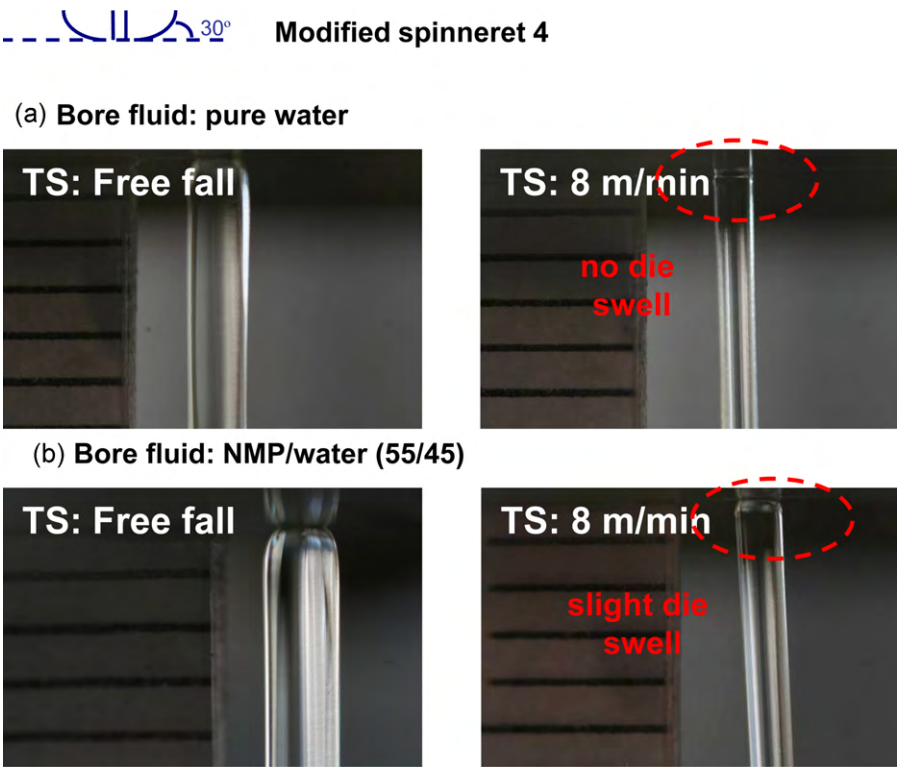

Fig. 12. The effects of increasing take-up speed (free fall and 8 m/min) on the die swell and flow stability of HPES hollow fiber spinning spun using modified spinneret 4 with: (a) bore fluid: pure water; (b) bore fluid: 55/45 wt% NMP/water.

the external work (or elongational stress) on the as-spun fibers [36,37,49–52]. This work (or stress) along spinning direction may counterbalance the instability force in the transversal direction, thus align the polymer chains in the spinning direction and suppress the flow instability and smoothen any distortion. As a result, it can be expected that less die swell and better flow stability can be achieved. However, the highest take-up speed that we could achieve using the stated spinning conditions is only 8 m/min. In the work by Yang et al. [24,25], the extensional viscosity characterizations show that hyperbranched polyethersulfone (HPES) has a more strain hardening effect due to its branched structure as compared to its linear counterpart. As a result, the HPES asymmetric film breaks more easily under high extensional strain and HPES hollow fiber has a weaker mechanical strength. This could be the reason why it is relatively difficult to achieve higher spinning speed in our work.

Fig. 11 illustrates the effects of take-up rate on die swell and flow instability in HPES hollow fiber spinning using various spinneret designs and pure water as a bore fluid. When a higher take-up speed spinning is carried out, both die swell and flow instability can be reduced prominently. This tendency applies for all spinneret designs as stated in Fig. 11. As an exception, modified spinneret 2 was not displayed in Fig. 11 because it originally did not show any die swell or flow instability at a low take-up rate as depicted in Fig. 8c.

Furthermore, a combination of high take-up speed spinning and non-solvent rich bore fluid composition shows an effective strategy to reduce die swell and enhance flow stability. In this case, modified spinneret 4 was chosen for further study. Fig. 12a displays their flow behavior where pure water was used as the bore fluid and the take-up rate was 8 m/min. The as-spun nascent fibers show no die swell as well as excellent flow stability. Fig. 12b shows that the fibers spun with NMP/water 55/45 wt% as bore fluid at a higher take-up rate exhibit a slight die swell with enhanced flow stability as compared to the fibers spun under free fall conditions. Clearly, a proper selection and combination of bore fluid composition, take-up speed and spinneret geometry is crucial in counteracting the die swell of spinning hyperbranch PES materials as well as enhancing their hollow fiber spinning stability.

4. Conclusion

The coupling effects of spinneret design modifications and spinning variables on the die swell effect and flow instability in the HPES and LPES hollow fiber spinning have been comprehensively investigated. A reduced die swell and improved flow stability can be accomplished by designing proper spinneret geometry together with adjusting spinning parameters. Hence, the following conclusions can be drawn from our study:

1. In terms of die swell effect, common spinneret and modified spinnerets 1, 3 and 4 result in less die swell for both LPES and HPES polymer solutions as compared to modified spinneret 2. However, in view of flow stability, modified spinnerets 2, 3 and 4 exhibit a relatively more stable flow as compared to other designs due to their lower stress inside the spinneret channel.
2. The effects of bore fluid composition on flow instability can be noticed prominently in the common spinneret and modified spinneret 1. It is found that there is a critical bore fluid composition to attain a more stable flow for the two corresponding spinneret designs. Interestingly, the bore fluid composition seems to have a little or no effect on the die swell in the HPES extrusion using common spinneret or modified spinnerets 1, 3 and 4. However, in the modified spinneret 2, the die swell effect transformation can be observed when the solvent in bore fluid is subsequently reduced from 95/5 wt% NMP/water to pure water.
3. The die swell and flow instability behavior become more apparent in all spinneret designs when the polymer dope flow rate increases from 1 to 5 ml/min since a higher dope flow rate generates a higher overall stress inside the spinneret.

4. Both die swell and flow instability significantly lessen with increasing spinning temperature in the HPES extrusion using the common spinneret and modified spinnerets 1 and 4.
5. A proper combination of high take-up speed spinning and non-solvent rich bore fluid composition can fully eliminate die swell and flow instability in the HPES hollow fiber spinning using the aid of modified spinnerets 3 and 4.

Acknowledgements

The authors would like to thank BASF SE, Germany for funding this research project with a grant number of R-279-000-283-597. We are also highly appreciated Dr. Q. Yang and Dr. K.Y. Wang for their help and suggestions on this work.

References

[1] J.R.A. Pearson, Y.T. Shah, Stability analysis of the fiber spinning process, J. Rheol. 16 (1972) 519.
[2] M. Shang, H. Matsuyama, M. Teramoto, D.R. Lloyd, N. Kubota, Preparation and membrane performance of poly(ethylene-co-vinyl alcohol) hollow fiber membrane via thermally induced phase separation, Polymer 44 (2003) 7441.
[3] S. Rajabzadeh, T. Maruyama, T. Sotani, H. Matsuyama, Preparation of PVDF hollow fiber membrane from a ternary polymer/solvent/nonsolvent system via thermally induced phase separation (TIPS) method, Sep. Purif. Technol. 63 (2008) 415.
[4] G.G. Lipscomb, The melt hollow fiber spinning process: steady-state behavior, sensitivity and stability, Polym. Adv. Technol. 5 (1994) 745.
[5] J.M. Piau, N.E. Kissi, B. Tremblay, Low Reynolds number flow visualization of linear and branched silicones upstream of orifice dies, J. Non-Newton. Fluid. Mech. 30 (1988) 197.
[6] T. Ishibashi, K. Aoki, T. Ishii, Studies on melt spinning of nylon 6. I. Cooling and deformation behavior and orientation of nylon 6 threadline, J. Appl. Polym. Sci. 14 (1970) 1597.
[7] T.H. Oh, M.S. Lee, S.Y. Kim, H.J. Shim, Studies on melt-spinning process of hollow fibers, J. Appl. Polym. Sci. 68 (1998) 1209.
[8] K.Y. Wang, T. Matsuura, T.S. Chung, W.F. Guo, The effects of flow angle and shear rate within the spinneret on the separation performance of poly(ethersulfone) (PES) ultrafiltration hollow fiber membranes, J. Membr. Sci. 240 (2004) 67.
[9] H.A. Tsai, C.Y. Kuo, J.H. Lin, D.M. Wang, A. Deratani, C. Pochat-Bohatier, K.R. Lee, J.Y. Lai, Morphology control of polysulfone hollow fiber membranes via water vapor induced phase separation, J. Membr. Sci. 278 (2006) 390.
[10] T.S. Chung, Z.L. Xu, W.H. Lin, Fundamental understanding of the effect of air-gap distance on the fabrication of hollow fiber membranes, J. Appl. Polym. Sci. 72 (1999) 379.
[11] N. Peng, T.S. Chung, J.Y. Lai, The rheology of Torlon® solutions and its role in the formation of ultra-thin defect-free Torlon® hollow fiber membranes for gas separation, J. Membr. Sci. 326 (2009) 608.
[12] T.S. Chung, S.K. Teoh, X. Hu, Formation of ultrathin high-performance polyethersulfone hollow fiber membranes, J. Membr. Sci. 133 (1998) 161.
[13] M.C. García-Payo, M. Essalhi, M. Khayet, Effects of PVDF–HFP concentration on membrane distillation performance and structural morphology of hollow fiber membranes, J. Membr. Sci. 347 (2010) 209.
[14] R.G. Larson, Instabilities in viscoelastic flows, Rheol. Acta 31 (1992) 213.
[15] C.J.S. Petrie, M.M. Denn, Instabilities in polymer processing, AIChE J. 22 (1976) 209.
[16] J.M. Piau, N.E. Kissi, B. Tremblay, Influence of upstream instabilities and wall slip on melt fracture and sharkskin phenomena during silicones extrusion through orifice dies, J. Non-Newton. Fluid. Mech. 34 (1990) 145.
[17] R.H. Moynihan, D.G. Baird, R. Ramanathan, Additional observations on the surface melt fracture behavior of linear low-density polyethylene, J. Non-Newton. Fluid. Mech. 36 (1990) 255.
[18] Y.E. Santoso, T.S. Chung, K.Y. Wang, M. Weber, The investigation of irregular inner-skin morphology of hollow fiber membranes at high speed spinning and the solutions to overcome it, J. Membr. Sci. 282 (2006) 383.
[19] S. Bonyadi, T.S. Chung, Investigation of corrugation phenomenon in the inner contour of hollow fibers during the non-solvent induced phase-separation process, J. Membr. Sci. 299 (2007) 200.
[20] W. Nijdam, J. de Jong, C.J.M. van Rijn, T. Visser, L. Versteeg, G. Kapantaidakis, G.-H. Koops, M. Wessling, High performance micro-engineered hollow fiber membranes by smart spinneret design, J. Membr. Sci. 256 (2005) 209.
[21] N. Widjojo, T.S. Chung, The thickness and air-gap dependence of macrovoid evolution in phase-inversion asymmetric hollow fiber membranes, Ind. Chem. Eng. Res. 45 (2006) 7618.
[22] H.K. Nason, A high temperature-high pressure rheometer for plastics, J. Appl. Phys. 16 (1945) 338.
[23] G. Pomar, S.J. Muller, M.M. Denn, Extrudate distortions in linear low-density polyethylene solutions and melt, J. Non-Newton. Fluid. Mech. 54 (1994) 143.
[24] Q. Yang, T.S. Chung, S.B. Chen, M. Weber, Pioneering explorations of rooting causes for morphology and performance differences in hollow fiber kidney dialysis membranes spun from linear and hyperbranched polyethersulfone, J. Membr. Sci. 313 (2008) 190.
[25] Q. Yang, T.S. Chung, M. Weber, K. Wollny, Rheological investigations of linear and hyperbranched polyethersulfone towards their as-spun phase inversion membranes' differences, Polymer 50 (2009) 524.
[26] J.L. den Otter, Some investigations of melt fracture, Rheol. Acta. 10 (1971) 200.
[27] F.A. Morrison, Understanding Rheology, Oxford University Press, New York, 2001, pp. 178–179.
[28] B. Voit, New developments in hyperbranched polymers, J. Polym. Sci. A: Polym. Chem. 38 (2000) 2505.
[29] Y.H. Kim, Hyperbranched polymers 10 years after, J. Polym. Sci. A: Polym. Chem. 36 (1998) 1685.
[30] C. Gao, D. Yan, Hyperbranched polymers: from synthesis to applications, Prog. Polym. Sci. 29 (2004) 183.
[31] S.E. Stiriba, H. Kautz, H. Frey, Hyperbranched molecular nanocapsules: comparison of the hyperbranched architecture with the perfect linear analogue, J. Am. Chem. Soc. 124 (2002) 9698.
[32] S.Y. Kwak, D.U. Ahn, Processability of hyperbranched poly(ether ketone)s with different degrees of branching from viewpoints of molecular mobility and comparison with their linear analogue, Macromolecules 33 (2000) 7557.
[33] T.S. Chung, J.J. Qin, J. Gu, Effect of shear rate within the spinneret on morphology, separation performance and mechanical properties of ultrafiltration polyethersulfone hollow fiber membranes, Chem. Eng. Sci. 55 (2000) 1077, and 56 (2001) 5869.
[34] J.J. Qin, J. Gu, T.S. Chung, Effect of wet and wet-jet spinning on the shear-induced orientation during the formation of ultrafiltration hollow fiber membranes, J. Membr. Sci. 182 (2001) 57.
[35] T.S. Chung, S.K. Teoh, W.W.Y. Lau, M.P. Srinivasan, Effect of shear stress within the spinneret on hollow fiber membrane morphology and separation performance, Ind. Eng. Chem. 37 (1998) 3930, and the subsequent correction. Ind. Eng. Chem. 37 (1998) 4903.
[36] S.J. Shilton, G. Bell, J. Ferguson, The rheology of fiber spinning and the properties of hollow fiber membranes for gas separation, Polymer 35 (1994) 5327.
[37] C. Cao, T.S. Chung, S.B. Chen, Z.J. Dong, The study of elongation and shear rates in spinning process and its effect on gas separation performance of poly (ethersulfone) (PES) hollow fiber membranes, Chem. Eng. Sci. 59 (2004) 1053.
[38] R.B. Bird, R.C. Armstrong, O. Hassager, Dynamics of Polymeric Liquids Fluid Mechanics, vol. 1, 2nd ed., John Wiley and Sons, 1987 (Chapter 4).
[39] N. Widjojo, T.S. Chung, W.B. Krantz, A morphological and structural study of Ultem/P84 copolyimide dual-layer hollow fiber membranes with delamination-free morphology, J. Membr. Sci. 294 (2007) 132.
[40] F.N. Cogswell, Converging flow of polymer melts in extrusion dies, Polym. Eng. Sci. 12 (1972) 64.
[41] J.R.A. Pearson, Mechanics of Polymer Processing, Elsevier Applied Science Publishers, London, 1985, p. 190.
[42] M.J. Crochet, A.R. Davies, K. Walters, Numerical Simulation of Non-Newtonian Flow, Elsevier, New York, 1984, p. 236.
[43] Y. Su, G.G. Lipscomb, H. Balasubramanian, D.R. Lloyd, Observations of recirculation in the bore fluid during hollow fiber spinning, AIChE 52 (2006) 2072.
[44] X.T. Yang, Z.L. Xu, Y.M. Wei, Two-dimensional simulation of hollow fiber membrane fabricated by phase inversion method, J. Appl. Polym. Sci. 100 (2006) 2067.
[45] A. De Rovere, R.L. Shambaugh, Melt-spun hollow fibers: modeling and experiments, Polym. Eng. Sci. 41 (2001) 1206.
[46] S.P. Rwei, Formation of hollow fibers in the melt-spinning process, J. Appl. Polym. Sci. 82 (2001) 2896.
[47] L.Y. Jiang, T.S. Chung, D.F. Li, C. Cao, S. Kulprathipanja, Fabrication of Matrimid/polyethersulfone dual-layer hollow fiber membranes for gas separation, J. Membr. Sci. 240 (2004) 91.
[48] N. Peng, T.S. Chung, The effects of spinneret dimension and hollow fiber dimension on gas separation performance of ultra-thin defect-free Torlon® hollow fiber membrane, J. Membr. Sci. 310 (2008) 455.
[49] T.S. Chung, The limitations of using Flory–Huggins equation for the states of solutions during asymmetric hollow fiber formation, J. Membr. Sci. 126 (1997) 19.
[50] S.J. Shilton, G. Bell, J. Ferguson, The deduction of fine structural details of gas separation hollow fiber membranes using resistance modeling of gas permeation, Polymers 37 (1996) 485.
[51] M.C. Porter, Handbook of Industrial Membrane Technology, Noyes Publications, NJ, USA, 1990, p. 153.
[52] M.C. Yang, M.T. Chou, Effect of post-drawing on the mechanical and mass transfer properties of polyacrylinitrile hollow fiber membranes, J. Membr. Sci. 116 (1996) 279.